Elastic Scattering of 30.3 MeV & 40 MeV Neutrons

R.P. DeVito, S.M. Austin, U.E.P. Berg, L.E. Young, J. Narayanaswamy

The isospin and energy dependence of the nucleon-nucleus optical-model potential (OMP) is being studied by elastic scattering of 30.3 MeV and 40 MeV neutrons. This work is intended to provide accurate neutron elastic scattering data at energies where such data are not available. This data should provide a better understanding of the energy dependence of the neutron-nucleus OMP from 11 to 40 MeV when combined with existing data.[1] Comparison with existing proton data at related energies will provide information on the isospin dependence of the nucleon-nucleus OMP.

The reaction ^{7}Li(p,n)^{7}Be(0,0.429) is used as a neutron source. With the neutron source 17.5 cm from the scattering sample a neutron flux of about 10^{8}n/cm^{2}/sec is obtained for a neutron energy spread of 500 KeV. The neutron source is positioned off the rotation axis of the beam swinger.[2] A 300 kg iron shield is positioned by remote control to prevent source neutrons from reaching the detector directly. The neutron detectors are located in a separate room from the neutron source, thus achieving good shielding. The region around the scattering sample that is visible to the detector is filled with Helium to minimize air scattering background.

Two cylindrical (10 cm dia. x 7.5 cm long) liquid scintillation detectors (NE 213) are operated side by side. This detector geometry allows for good angular resolution of the scattered neutrons (typically <0.5°) and for tight shielding between the source and the detector room. Each detector provides pulse-shape discrimination (PSD), recoil energy (light), as well as time-of-flight information. The data is collected using a PDP 11/45 computer and a versatile program that allows several TOF spectra with different light and PSD gates.

The monitor detector is a much smaller (2 cm dia. x 1.5 cm long) solid organic scintillator (NE102) which rotates with the beam swinger and detects 40° neutrons from the Li target. The monitor also views a light-emitting-diode triggered by a temperature compensated pulser to produce a reference peak in the light spectrum, permitting one to detect any gain shifts and to accurately correct for dead time. Gain shift monitoring is important because count rates change by a factor larger than 100 during the experiment.

Angular distributions for the elastic scattering of 30.3 MeV neutrons from 20° to 130° have been measured for natural targets of C, Si and S. These targets contain 99%, 92% and 95% T=0 components in their natural abundances, respectively. In all cases, the ground state was cleanly resolved from the first excited state. Fig. 1 shows the time-of-flight (TOF) spectrum for 30.3 MeV neutrons on Si at 40°. The elastic peak has its centroid at channel 625 while the scattering from the 2+ state at 1.78 MeV excitation has its centroid at channel 588. Fig. 2 shows the angular distribution for 30.3 MeV neutrons scattered from S^{32}.

1. J. Rapaport et al., Nucl. Phys. A286, (1977) 232.

2. R.J. Bhowmik et al., N.I.M. 143, (1977) 63.

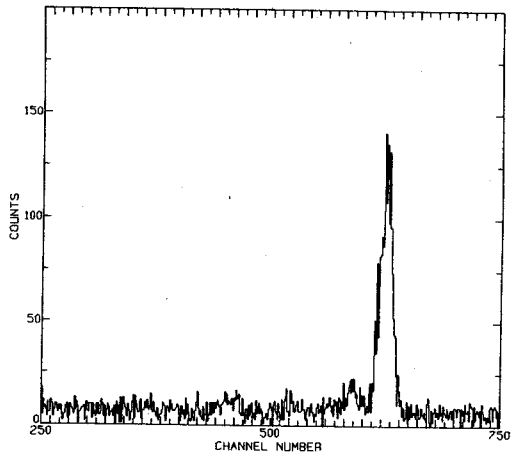

Fig. 1. Time-of-flight spectrum for 30.3 MeV neutrons on Si at 40°. Baseline is at 5 counts per channel to achieve accurate background subtraction.

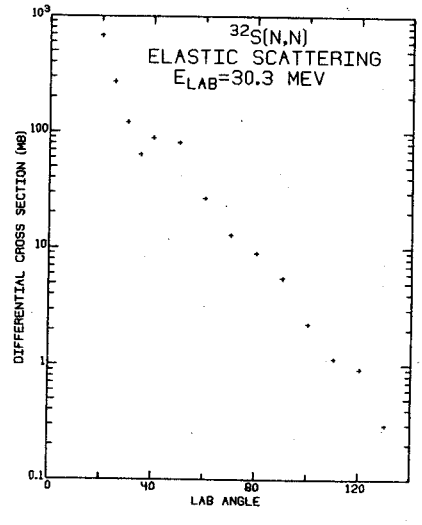

Fig. 2. Preliminary differential cross section for elastic scattering of 30.3 MeV neutrons from natural sulfur.

Cross Section Ratios for Elastic Proton Scattering

S. Austin, C. King, E. Kashy, R. Markham, I. Redmount, S. Motzny, and R. Ronningen

We are now beginning the theoretical analysis of cross section data from the elastic scattering of 30.3 MeV protons from a mixed Ca metal target.[1] Elastic scattering cross section ratios of ^{44}Ca and ^{48}Ca relative to ^{40}Ca were determined for 32 angles in the angular range of 32° to 126°. From the Coulomb-scattering of ^{12}C ions, the relative abundances of ^{40}Ca, ^{44}Ca, and ^{48}Ca in the target were determined to be 1.000, 0.929, and 0.806 (all ±3%), respectively. Absolute cross sections for each isotope were then obtained by normalizing the ^{40}Ca relative cross section data to the absolute cross section data of Ridley and Turner.[2]

Our initial theoretical analysis of the data is based on standard optical model searches, using the search code GIBELUMP. We are obtaining good fits (χ^2/point≈0.5) with parameter values which include a small, positive imaginary part (i.e., the same sign as the real part) to the spin-orbit potential. The measured cross section ratios and the optical model predictions are shown in the figure.

We are also fitting the elastic scattering data for ^{40}Ca with the polarization data of Hnizdo et al.[3] included. Upon the completion of standard optical model searches for each isotope, we hope to determine the parameters of the "model independent" potential which must be added to the ^{40}Ca potential to fit the cross-section ratios.

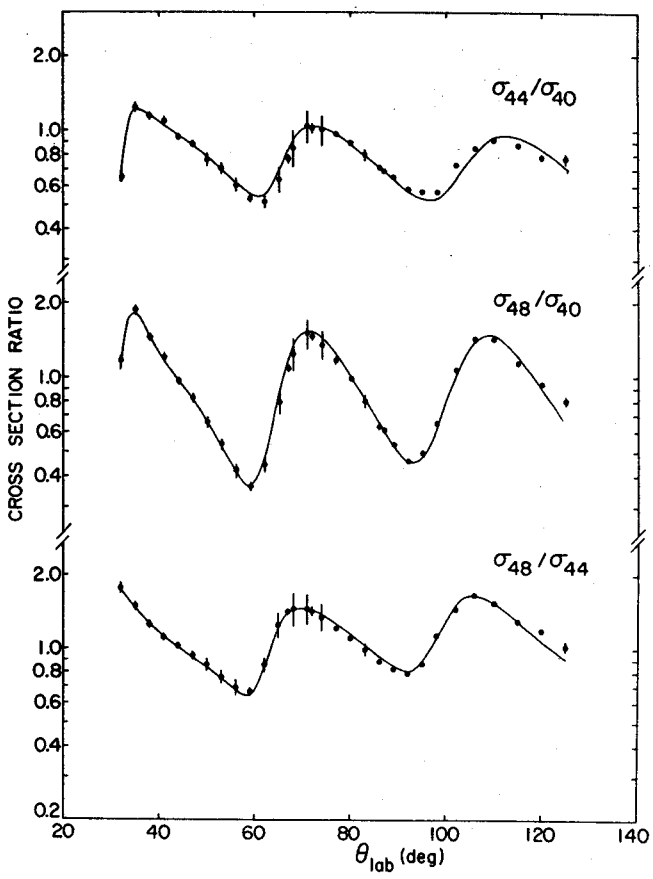

Fig. 1

1. S. Austin et al., MSU Annual Report 1976-1977, p. 26.
2. B.W. Ridley and J.F. Turner, Nucl. Phys. 58, 497 (1964).
3. V. Hnizdo et al., Phys. Rev. C3, 1560 (1971).

Elastic Scattering of ^{6}Li at 75 MeV

R. Huffman, A. Galonsky, C. Williamson, and R.G. Markham

In this study, measurements of ^{6}Li elastic scattering for a range of targets are being made. Similar data at lower energies are available from other groups.[1] Thus, these studies will allow us to learn of the simultaneous mass and energy dependence of the optical model parameters for ^{6}Li.

Data have been obtained for angles up to 50° for targets of ^{58}Ni, ^{90}Zr, ^{124}Sn, and ^{208}Pb. These measurements were made with two surface barrier detector telescopes symmetrically placed on opposite sides of the beam axis. This symmetry was used to monitor proper beam alignment and to improve the statistical accuracy of the large angle runs. Pulses from both telescopes were processed in the same octal ADC and were, thus, subject to the same system dead-time.

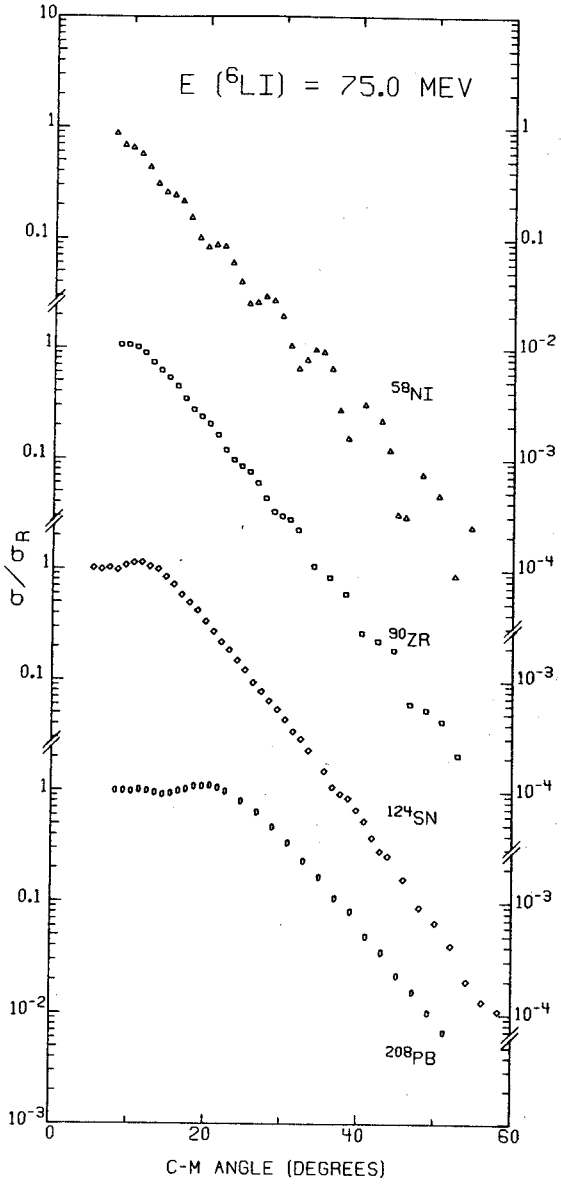

Fig. 1. Elastic scattering data for ^{6}Li at an incident energy of 75 MeV on targets of ^{58}Ni, ^{90}Zr, ^{124}Sn, and ^{208}Pb.

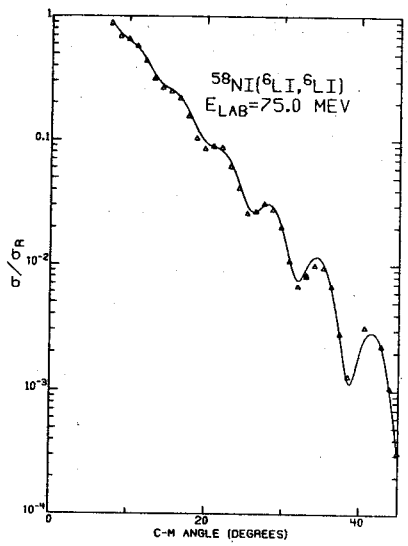

Fig. 2. Elastic scattering data for ^{58}Ni (^{6}Li,^{6}Li) at an incident energy of 75 MeV. The curve is the result of calculations using the parameters of Table I.

The optical model analyses are being carried out using the computer code SGIBELUMP. The accuracy parameters of SGIBELUMP are being investigated. These include the number of partial waves included in the scattering matrix, the radius for the matching of the internal solution of the Schrodinger equation with the asymptotic solution, and the step size for the integration of the internal solution. A comparison of the results from SGIBELUMP is being made with the results from the DWBA computer code DWUCK.

In the optical model analyses, both the real and the imaginary wells are volume potentials of the Woods-Saxon form. Gridding is being done on the real well depth. The imaginary well depth and the geometry parameters are allowed to vary independently. Gridding on the real well depth will reveal the discrete families of parameters.

Figure 1 shows the data that have been taken for all four targets. Figure 2 shows the data for ^{58}Ni to 42° (lab frame) and a fit from preliminary gridding searches using the parameters in Table I.

Table I

V_R (MeV)	r_R (fm.)	a_R (fm.)	V_I (MeV)	r_I (fm.)	a_I (fm.)
180.	1.40	0.59	23.3	1.52	1.13

1. R.I. Cutler, M.J. Nadworny, and K.W. Kemper, Phys. Rev. C15 (1977) 1318; L.T. Chua, F.D. Becchetti, J. Jänecke, and F.L. Milder, Nucl. Phys. A273 (1976) 243; C.M. Perey and F.G. Perey, Atom. Data and Nucl. Data Tables 17 (1976) 1-101

Determination of Radii for ^{1}H, ^{3}He, and ^{4}He Determined from Elastic e^{-} Scattering

J. Borysowicz

We use a recently developed method[1] to determine densities and radii for protons, ^{3}He and ^{4}He. We derive the error terms for the frequently used formula $r^2 = -3f''(0)$. The difference with the other methods is that we rely nearly entirely on experiment. We do not use models with a physical content. The assumptions that we make are weak and are expressed entirely in terms of the density at large distances and the form factor at large momentum transfers. In spite of the weak assumptions, the accuracy of our determination is comparable to the accuracy obtained with physical models.

For ^{3}He and ^{4}He the experimental results are such that the charge densities and radii are determined well. For protons the present experimental information allows for good determination of the magnetic density and radius.

---

1. J.R. Borysowicz and J.H. Hetherington, to be published in Nuclear Physics; J.R. Borysowicz and J.H. Hetherington, Bull. Amer. Phys. Soc. 23 (1978) 519.

L-Dependent Optical Potentials and DWBA Calculations of (p,p')

R.S. Mackintosh*

It has been shown by Kobos and Mackintosh[1] that a considerable volume of elastic proton scattering data for lighter nuclei can be fitted very well with an explicitly ℓ-dependent optical potential. The properties of this appear to be related to channel coupling effects, and the parameters exhibit rather systematic behaviour. However, elastic scattering alone cannot finally prove the correctness of the ℓ-dependence hypothesis. It seemed worthwhile to see whether this new OM leads to nucleon wave functions sufficiently different within the nucleus to lead to differences in DWBA calculations of (p,p'). Indeed, it is ultimately the influence of such effects upon spectroscopically useful reactions such as (p,p') that makes the phenomenon most worthy of study.

There are two aspects of the application of ℓ-dependent potentials to (p,p'). One is simply to calculate the partial waves with ℓ-dependent optical potentials. The second is to apply the general ℓ-dependent idea to the inelastic scattering form factor. Even the first is not without ambiguity since the ℓ-dependent terms are certainly local-equivalents to non-local terms of some complexity. We have no way of knowing what kind of "Perey effect" might be present. The second aspect is subject to many ambiguities since there is a greater variety of coupling terms than those determined by elastic scattering. The ℓ-dependence comes from "higher order terms," and the relationship between those for diagonal (i.e. OM) and non-diagonal (inelastic coupling) is not really known; it is precisely the question of two-step processes and these can affect the couplings to different states differently. This investigation is mainly confined to determining whether the use of the very different ℓ-dependent OM makes a substantial difference to inelastic scattering. We emphasize that our potential fits the elastic scattering data very well. Previous comparisons of DWBA calculations with different OM parameters have led to the conclusion that there is little effect on (p,p') cross sections. This is because the compared potentials were both related to similar global sets which did not really fit the elastic scattering data for the nucleus in question, ^{16}O.

We modified DWUCK to include the ℓ-dependent OM of Kobos and Mackintosh.[1] We have optical potentials which fit the data at 30.1 and 24.5 MeV and we used these in a calculation of the excitation at the 6.13 MeV 3^- state with small mismatch of exit proton energy. The comparison ℓ-independent potentials are also given in Kobos and Mackintosh. The inelastic scattering was generated with real and complex macroscopic form factors which were the derivatives of neither of the optical potentials, but our comparison should give a reasonable indication of the importance of the OM in a microscopic calculation with independently fixed form factors.

In Fig. 1 we show the results with real and complex (with imaginary part peaked further out) form factors. Very large effects are seen at angles forward of the maximum and at back angles. As was the case for elastic scattering, we have a clear counter-example to the belief that backward angle peaking is a necessary indication of resonance contributions (which may still be present, of course).

As has been shown by v. Geramb and Hodgson,[2] detailed fits to $d\sigma/d\theta$ out to 100^o may be achieved by using a general fitted complex form factor. We have not attempted such calculations. Although the backward angle peak we get is qualitatively different to that of the data of Austin et al.,[3] we note that the fitted complex form factors[2] have a profound effect at backward angles also, without fitting the data. Our results imply that since ℓ-dependent potentials would make further large changes to these angular distributions the effects of using these upon parameters extracted from more elaborate DWBA calculations deserves study. ℓ-dependent potentials will certainly modify the extraction of resonance phenomena.

We also studied ℓ-dependent excitation form factors and these gave considerable freedom for adjusting the details of angular distributions. A theory providing a reliable prescription for possible ℓ-dependent form factors is badly needed.

* On leave from Daresbury Laboratory, Warrington, England.

1. A.M. Kobos and R.S. Mackintosh, J. Phys. G. to be published, Daresbury preprint.
2. H.V. v. Geramb and P.E. Hodgson, Nucl. Phys. A246 (1975) 173.
3. S.M. Austin et al., Phys. Rev. C 3 (1971) 1514.

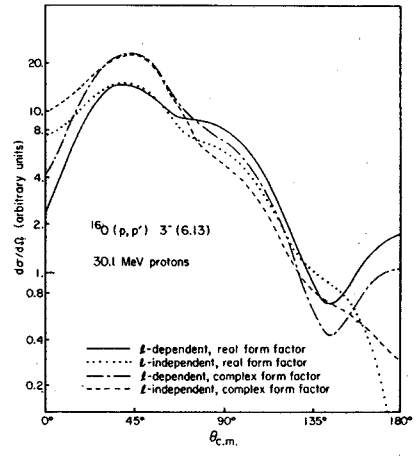

Fig. 1. Inelastic scattering of 30.1 MeV protons to the 6.13 MeV 3^- state of ^{16}O comparing results obtained with ℓ-dependent and ℓ-independent optical potentials of ref. 1 for both real and complex excitation form factors.

Inelastic Proton Scattering from ^{12}C and ^{14}N at 122 MeV

J. Comfort,* S.M. Austin, P. Debevec,** G. Moake,+ R. Findlay,++ and W.G. Love†

The states of ^{12}C and ^{14}N provide a convenient testing ground for reaction mechanisms in inelastic scattering since their quantum numbers allow one to conveniently isolate the contributions of various parts of the effective two nucleon interaction V_{ip} (here p denotes the projectile and i a valence nucleon). Thus, if one writes the central part of V_{ip} as

$$V_{ip}=V_o+V_\sigma\vec{\sigma}_i\cdot\vec{\sigma}_p+V_\tau\vec{\tau}_i\cdot\tau_p+V_{\sigma\tau}(\vec{\sigma}_i\cdot\vec{\sigma}_p)(\vec{\tau}_i\cdot\vec{\tau}_p)$$

one expects transitions to the 4.44 MeV (2^+,T=0), 12.71 MeV (1^+,T=0), 15.1 MeV (1^+, T=1), and 16.11 MeV (2^+,T=1) states of ^{12}C to be mediated dominantly by V_o, V_σ, $V_{\sigma\tau}$, and V_τ respectively.[1] The (1^+,T=0→0^+,T=1) transition to the first excited 2.31 MeV state in ^{14}N is a special case. While one might expect this transition to be dominated by the central interaction $V_{\sigma\tau}$, the same wavefunction accident responsible for the great inhibition of the β decay of ^{14}C weakens the L=0 contribution of the central force, allowing the tensor force to dominate.

The measurements were performed with a 122 MeV proton beam at the Indiana University Cyclotron Laboratory. Targets consisted of ^{12}C and melamine foils for the ^{12}C and ^{14}N experiments respectively. Preliminary experimental and theoretical results for ^{12}C were presented in the 1978 Indiana progress report and will only be briefly summarized here. Calculations (including knock-on exchange) using the impulse approximation effective interaction of Love et al.[2] and the wavefunctions of Cohen and Kurath (6-16 2BME) were reasonably successful in reproducing the data to the 4.44 MeV, 15.1 MeV, and 16.1 MeV states, although the magnitude of the predicted cross section for the latter state is somewhat uncertain because the uncertainty in B(E2) for this state leads to an uncertainty in the effective charge associated with the Cohen-Kurath wavefunctions. The cross section for the 12.71 MeV state is, for presently unknown reasons, very poorly described.

Cross sections for elastic and inelastic scattering on ^{14}N were obtained between 5.5° and 52°. Normalizations by comparison of the inelastic scattering to ^{12}C (4.44) present in the same spectrum and by use of a thick BN target were in good agreement. A DWBA calculation for the 2.31 MeV transition (1^+_0→0^+_1) made using Cohen-Kurath (6-16 2BME) wavefunctions and the same impulse approximation force as for ^{12}C reproduces the general magnitude of the cross section at the most forward angles but was too large by as much as a factor of four near a secondary maximum at 30°. In addition, the diffraction structure of the calculated cross section is shifted to smaller angles compared to the data. The sensitivity of this cross section to the details of the calculation is under investigation.

---

* University of Pittsburgh, Pittsburgh, PA 15260.
** University of Illinois, Urbana, IL 61820.
+ Indiana University, Bloomington, IN 47401.
++ Ohio University, Athens, OH 45701
† University of Georgia, Athens, GA 30602.

1. S.M. Austin, The Two Body Force in Nuclei, Plenum Press, p. 285.
2. W.G. Love et al, Phys. Lett. 73 (1978) 277.

Inelastic Scattering of 40 MeV Protons on s-d Shell Nuclei

B. Zwieglinski, J.A. Nolen, G.M. Crawley, and J. Finck

Due to recent progress in nuclear shell-model calculational techniques,[1] the wavefunctions of the 2sld-shell nuclei calculated in the complete 2sld-shell basis are presently available.[2] The predictions of these calculations have been compared with the traditional spectroscopic observables such as static and transition electromagnetic moments, beta decay log ft values, and single nucleon spectroscopic factors. Another test of these wavefunctions is in the calculation of the nucleon inelastic scattering cross sections using a microscopic reaction theory. The present microscopic DWBA theory incorporating nucleon exchange[3] and utilizing realistic[4] (i.e. derived from the free nucleon-nucleon force) two-body interaction alows an experimental test of the shell-model wavefunctions of similar quality as that offered by inelastic electron scattering, for example. Therefore a high-resolution study of the inelastic proton scattering on nuclei from the middle of sd shell was undertaken at E_p=40 MeV. At present the study of ^{24}Mg has been completed[5,6] and the study of ^{28}Si is in progress. Measurements on ^{26}Mg and ^{32}S are planned.

The main conclusions from the ^{24}Mg(p,p')^{24}Mg study[6] are the following. The large basis shell-model and DWBA account quite well for most transitions in which one-step excitation dominates. It should be stressed that transitions differing by three orders of magnitude in cross section have been encountered in this work. Enhancement factors extracted for the natural parity transitions are consistent with the effective charges obtained from the electromagnetic transition rates. Levels corresponding to the giant M1 resonance in ^{24}Mg have been resolved in this experiment. The fact that the normalization factor between theory and experiment is close to unity for the 10.713 MeV 1^+; T=1 state indicates that little or no renormalization of the two-body force is necessary for this inelastic transition. The normalization factors close to unity are found also for magnetic-type transitions of multipolarities higher than M1, suggesting that little core-polarization effect may be involved in other magnetic-type transitions. No electromagnetic data for these transitions exist at present.

One of the significant results of this work is the interpretation of the differences between the shapes of the angular distributions for the 1.567 MeV and 4.239 MeV 2^+ states and the angular distribution for the 2^+ state at 7.348 MeV (see Fig. 1), the former two decreasing more rapidly with angle. This indicates qualitatively that the transition density for the latter state is concentrated at smaller radii. Shell-model calculations suggest that this is the result of cancellation in the surface region of the density for the transitions between the 2s and the 1d orbitals (dashed lines in the insets to Fig. 1) and the density for the transitions between the 1d-orbitals (dash-and-dot lines). For the 1.369 MeV and 4.239 MeV states the partial densities add constructively, yielding the resulting density (solid lines) with a surface-peaked shape. Independently, Singhal et al.[7] gave an identical interpretation for the differences between the momentum transfer dependence of the inelastic electron scattering form-factors for the 2^+_1 and 2^+_2 states in ^{20}Ne.

1. R.R. Whitehead, A. Watt, B.J. Cole, and I. Morrison, in Advances in Nuclear Physics, ed. by M. Beranger and E. Vogt (Plenum Press, New York, 1977), vol. 9, p. 125.
2. W. Chung and B.H. Wildenthal (to be published).
3. R. Schaeffer and J. Raynal, code DWBA 70 (unpublished).
4. G. Bertsch, J. Borysowicz, H. McManus, and W.G. Love, Nucl. Phys. A284 (1977) 399.
5. B. Zwieglinski, G.M. Crawley, H. Nann, and J.A. Nolen, Jr., Phys. Rev. C 17 (1978) 872.
6. B. Zwieglinski, G.M. Crawley, W. Chung, H. Nann, and J.A. Nolen, Jr., Report MSUCL-263, April 2978 and Phys. Rev. C (to be published).
7. R.P. Singhal, R.G. Arthur, E.A. Knight, M.W.S. Macauley, D. Kelvin, A. Watt, and R.R. Whitehead, Phys. Lett. 76B (1978) 170.

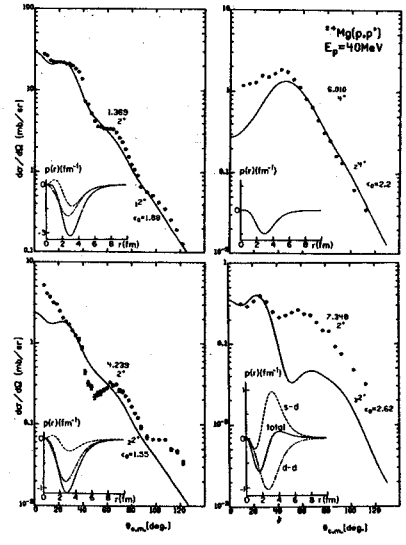

Fig. 1. Experimental and microscopic DWBA angular distributions for selected natural parity, T=0 states in ^{24}Mg. The isoscalar enhancement factors (ϵ_0) are indicated. In the insets the microscopic transition densities for the transitions between s and d orbitals (dashed lines), between d orbitals (dash-and-dot) and total densities (solid lines) are presented.

Inelastic Proton Scattering on ^{34}S

U.E.P. Berg, G.M. Crawley, and B. Zwieglinski

Very little information about excited states in the energy region above 8 MeV in ^{34}S is given in the literature. We have performed $^{34}S(p,p')$ measurements to test excitation energies and spin assignments obtained in a recent $^{34}S(\gamma,\gamma)$ experiment.[1]

The $^{34}S(p,p')$ experiment has been carried out with a 40 MeV proton beam and an 80 $\mu g/cm^2$ thick ^{34}S target of the sandwich type described in Ref. 2. After each run on the enriched ^{34}S target a second measurement on natural S was performed to determine background peaks from the ^{32}S impurity. The protons were momentum analysed in the Enge split-pole spectrometer and detected in the focal plane by a 50 cm long position sensitive proportional counter with delay line readout backed by a plastic scintillator. Additional runs on photographic plates were taken to obtain more precise excitation energies for the states observed. Cross sections were measured at 15°, 30°, 40°, 50°, and 60°.

Fig. 1 shows a part of a measured $^{34}S(p,p')$ spectrum together with a $^{32}S(p,p')$ spectrum. Both spectra were taken with the proportional counter, one after the other at the same proton energy of 42 MeV and a scattering angle of 30°. The broad background beginning at 9 MeV excitation energy stems from elastic proton scattering on hydrogen contained in the formvar layer of the sulfur target cover and backing. This background peak is shifted to a higher excitation energy region at large scattering angles. The peaks are labeled with the corresponding excitation energies in keV and background peaks are hatched. Peaks labeled with a star were used for energy calibration.

The ^{34}S energies determined from a comparison with ^{32}S agree within 3 keV with energies observed in nuclear resonance fluorescence.[1] Table I gives a comparison of states observed in this experiment with previous data in the energy range from 7.4 to 10.0 MeV. The energies in Table I have been obtained from the spectra on plates for which the energy resolution was 10 keV. Nineteen levels in Table I have not been observed previously. In comparison to the resonance fluorescence experimental states with $J^\pi=1^-$ show up relatively strongly but transitions to states with 1^+ (unnatural parity) are very weak in $^{34}S(p,p')$.

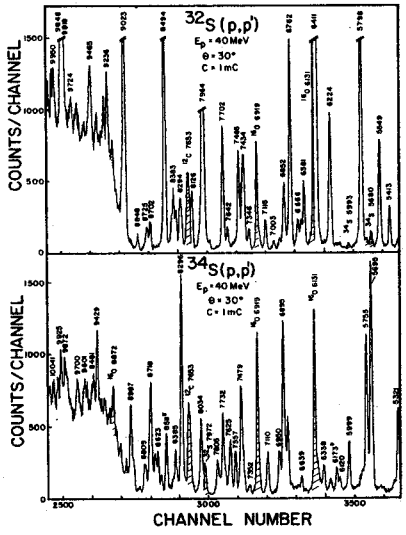

Fig. 1. Delay-line counter spectra of $^{32}S(p,p')$ and $^{34}S(p,p')$.

1. U.E.P. Berg, K. Bangert, G. Junghans, R. Stock, and K. Wienhard, Nucl. Phys. (in print).
2. M.A. Hedemann, Nucl. Inst. and Meth. 141 (1977) 377.
3. P.M. Endt and C. van der Leun, private communication.
4. P.M. Endt and C. van derLeun, Nucl. Phys. (1967) 105.

Table I. Comparison of excitation energies from $^{34}S(p,p')$ with published data.

E_x(keV)[a]	J^π[a]	Resonance fluorescence E_x(keV)[b]	J^π[b]	This work $^{34}S(p,p')$ E_x(keV)
7476 ± 10				7479 ± 5
7548 ± 10				7557 ± 5
7630 ± 7	3^-			7625 ± 5
7655 ± 9				
7714 ± 15				
7735 ± 9				7732 ± 5
7753 ± 9	$(0-3)^-$			
7784 ± 9	$(0-3)^-$	7781 ± 2	1^-	7779 ± 5
7801 ± 11	2^+			7805 ± 5
7971 ± 15				7976 ± 5
8025 ± 15	0^+			8034 ± 5
8142 ± 12	$(0-3)^-$			
		8185 ± 3	(1^+)	
8255 ± 15				
8296 ± 10				8296 ± 5
8383 ± 15	1^-	8385 ± 3	(1^-)	8385 ± 5
8418 ± 11	4^+			8423 ± 5
8496 ± 15	1^-	8511 ± 3	1^-	8511 ± 5
				8580 ± 5
				8623 ± 5
		8657 ± 7	(1^+)	8656 ± 5
				8671 ± 5
				8718 ± 5
				8740 ± 10
				8792 ± 5
				8809 ± 5
				8953 ± 5
				8987 ± 5
				9120 ± 5
				9171 ± 5
				9205 ± 7
				9226 ± 6
				9257 ± 10
				9429 ± 5
				9445 ± 5
		9478 ± 4	1	9481 ± 5
				9566 ± 10
				9601 ± 5
		9640 ± 4	(1^+)	-----
		9711 ± 5	(1^+)	9700 ± 6
				9847 ± 10
		9860 ± 7	(1^+)	9872 ± 5
9927[c]				9925 ± 5
9976[c]				9969 ± 10

[a] Ref. 3
[b] Ref. 2
[c] Ref. 4

Study of the Particle-Core Coupling in ^{63}Cu by Proton Inelastic Scattering

Y. Iwasaki, G.M. Crawley, R.G. Markham, J.E. Finck, and J.H. Kim

The nucleus ^{63}Cu is a typical and classical example of the nuclei for which a theoretical interpretation of low-lying states has been given in a particle-core coupling picture. In this picture ^{63}Cu is considered to consist of one proton added to the proton-closed-shell nucleus ^{62}Ni which is called the core. The proton is generally assumed to occupy the $2p_{3/2}$, $2p_{1/2}$, and $1f_{5/2}$ orbitals in low-lying states of ^{63}Cu. Inelastic scattering of alpha particles,[1] protons,[2] and electrons[3] were considered to be effective means of selectively exciting collective degrees of freedom of the core. More recently, the ^{65}Cu(p,t)^{63}Cu reaction was used to study the quadrupole core-excited components of low-lying states in ^{63}Cu.[4,5] It is pointed out that the (p,t) reaction is even more selective than inelastic scattering in exciting the core-excited component of a particle-core-coupled state, since the (p,t) reaction does not change the state of the odd proton to the first approximation.[4]

Low-lying states in ^{63}Cu are interpreted as arising from the coupling of one proton in the $2p_{3/2}$, $2p_{1/2}$, and $1f_{5/2}$ orbitals with the 2_1^+ state of ^{62}Ni.[5,6] If a reaction process excites only one collective degree of freedom of the core (i.e. if only one collective operator acting on the core is involved), the relative cross sections for the particle-core-coupled states should be independent of the incident energy. There is an excellent agreement between the relative cross sections at E_p=19.5 MeV[5] and those at E_p=51.9 MeV[4] in the ^{65}Cu(p,t)^{63}Cu. On the other hand, incident-energy dependence of the relative cross sections has not been known experimentally for inelastic scattering. For proton inelastic scattering there was only one set of high-resolution data obtained at E_p=17.5 MeV.[2] There is a remarkable discrepancy between the relative cross sections observed in proton inelastic scattering[2] and those observed in the (p,t) reaction.[4,5] If the odd proton is a spectator, and if only one and the same type of collective core-excitation matrix element is involved in two different reaction processes, the relative cross sections for the particle-core-coupled states should be the same for the two reaction processes. Therefore there is apparently a problem regarding the mechanism of proton inelastic scattering. We have therefore undertaken a high-resolution proton inelastic scattering experiment on ^{63}Cu at an energy much higher than 17.5 MeV at which the only set of data was available.

We measured differential cross sections for proton inelastic scattering by ^{63}Cu at E_p=40 MeV. Protons were detected by a delay-line counter[7] placed at the focal plane of the Enge split-pole magnetic spectrograph. Other particles were rejected by means of time-of-flight signals and energy-loss signals. The target was a self-supporting metallic foil of ^{63}Cu with a thickness of 520 $\mu g/cm^2$. The overall energy resolution was 20 to 25 keV. Angular distributions were obtained in the angular range from 8° to 95° lab for a number of states up to an excitation energy of 4 MeV, and an assignment of the transferred angular momentum L was made to each of them. The results are summarized in Table I.

Table I. Experimental results. The values of E_x' and J^π are taken from the gamma-ray work of Ref. 10.

E_x (MeV)	E_x' (MeV)	J^π	$(d\sigma/d\Omega)^{cm}_{max}$ (mb/sr)	(θ^{cm}_{max}) (deg)	L
0.67	0.6696	$1/2^-$	2.4	(8.1)	2
0.96	0.9621	$5/2^-$	10.1	(8.1)	2
1.33	1.3270	$7/2^-$	10.1	(8.1)	2
1.41	1.4120	$5/2^-$	1.0	(8.1)	2
1.55	1.5470	$3/2^-$	0.64	(8.1)	2
1.86	1.8612	$7/2^-$	0.74	(8.1)	2+(4)
2.01	2.0112	$3/2^-$	0.37	(8.1)	2
2.08	2.0815	$5/2^-$	0.27	(8.1)	(2+4)
2.21	2.2080	$9/2^-$	0.22	(8.1)	4
2.34	2.3365	$5/2^-$	0.11	(8.1)	4
2.41	2.4048	$7/2^-$	0.15	(8.1)	(2+4)
2.51			1.95	(20.3)	3
2.54	2.5358	$5/2^-$	0.17	(8.1)	(4)
5.68			0.66	(8.1)	4
3.32			1.19	(20.3)	3
3.48			0.86	(20.3)	3
3.72			0.82	(20.3)	3
3.81			0.64	(20.3)	3
3.84			0.50	(20.3)	3
3.89			0.36	(20.3)	3

An energy dependence of the relative cross sections is observed for the low-lying states excited by ℓ=2 transitions, as shown in Table II. It is not very strong, however, and the difference between the relative cross sections in inelastic scattering and those in the (p,t) reaction persists at E_p=40 MeV. This seems to be associated with different reaction mechanisms of inelastic scattering and the (p,t) reaction.

In the region of higher excitation energies, we have found seven strong octupole transitions leading to states at E_x=2.51, 3.32, 3.48, 3.72, 3.81, 3.84, and 3.89 MeV. The levels at E_x=3.81, 3.84, and 3.89 MeV have been resolved for the first time. Five octupole transitions were reported by previous (α,α'), (p,p'), and (e,e') experiments.[1,2,3] Four of the final states were suggested to arise from the coupling of the $2p_{3/2}$

proton orbital with the octupole state of the core (the 3_1^- state at E_x=3.75 MeV in ^{62}Ni).[1,8] The state at E_x=2.51 MeV has a large component of the $1g_{9/2}$ proton orbital[9] and the strongly enhanced octupole transition to the state is a puzzle, for which an explanation has been offered recently.[8] The existence of seven octupole core-excited states instead of the five known so far suggests that a sophisticated particle-core-coupling model is needed for ^{63}Cu.

1. B.G. Harvey, J.R. Meriwether, A. Bussiere, and D.J. Horen, Nucl. Phys. 70 (1965) 305.
2. A.L. McCarthy and G.M. Crawley, Phys. Rev. 150 (1966) 935.
3. A.A.C. Klaasse, P.F.A. Goudsmit, and P.K.A. de Witt Huberts, in Problems of Vibrational Nuclei, ed. G. Alaga, V. Paar, and L. Sips, Fizika 7, Suppl. 2 (1975) 128.
4. Y. Iwasaki, M. Sekiguchi, F. Soga, and N. Takahashi, Phys. Rev. Lett. 29 (1972) 1528.
5. R.G. Markham and H.W. Fulbright, Nucl. Phys. A203 (1973) 244.
6. V.K. Thankappan and W.W. True, Phys. Rev. B137 (1965) 137; J.L. DeJager and E. Boeker, Nucl. Phys. A216 (1973) 349.
7. R.G. Markham and R.G.H. Robertson, MSUCL-173 (1975).
8. A.A.C. Klaasse and V. Paar, Nucl. Phys. A297 (1978) 45.
9. A.G. Blair, Phys. Rev. B648 (1975) 140; R.M. Britton and D.L. Watson, Nucl. Phys. A272 (1976) 91.
10. C.T. Papadopoulos, A.G. Hartas, P.A. Assimakopoulos, G. Andritsopoulos, and N.H. Gangas, Phys. Rev. C 15 (1977) 1987.
11. Y. Iwasaki, G.M. Crawley, R.G. Markham, J.E. Finck, and J.H. Kim, Annual Report 1977-78, Cyclotron Laboratory, Michigan State University (present volume).

Table II. Relative cross sections for low-lying states in ^{63}Cu. Summed cross sections are normalized to 1.00 for the $7/2_1^-$ state.

	^{65}Cu(p,t)^{63}Cu			^{63}Cu(p,p')^{63}Cu	
	19.5 MeV[a]	40 MeV[b]	52 MeV[c]	17.5 MeV[d]	40 MeV[e]
$1/2_1^-$	0.18	0.16	0.18	0.29	0.23
$5/2_1^-$	0.46	0.43	0.46	1.00	0.91
$7/2_1^-$	1.00	1.00	1.00	1.00	1.00
$5/2_2^-$	0.09	0.10	0.07	0.16	0.08

a. Ref. 5. b. Ref. 11 c. Ref. 4. d. Ref. 2.
e. Present work.

Nuclear Deformation Parameters of Lanthanide and Actinide Nuclei from Proton Inelastic Scattering

G.M. Crawley, J.E. Finck, J.A. Nolen, Jr., R. Melin, R. Ronningen, C.H. King, and C.E. Bemis, Jr.*

The determination of nuclear deformations is one of the most fundamental problems in the study of nuclear shapes. The lowest order (quadrupole) moments of static deformed nuclei have been fairly well established by various techniques, most notably through electromagnetic measurements. However, the determinations of hexadecapole and other higher-order nuclear deformations are particularly interesting because calculations have shown[1] that nuclear binding energies are quite sensitive to the presence of hexadecapole deformations. Thus, for example, the magnitude of the hexadecapole deformations in the actinide nuclei could have considerable bearing on whether long-lived superheavy nuclei exist[1].

The inelastic scattering of 35 MeV protons from heavy nuclei is sensitive mainly to the nuclear matter distribution and is quite insensitive to the charge distribution. Measurements on the lanthanide nuclei ^{154}Sm and ^{176}Yb and the actinides ^{232}Th and ^{238}U have been carried out with 35 MeV protons and a preliminary report on this work has been published[2].

Recent work has focused on three main directions. One is the determination of the errors associated with the parameters to allow a more meaningful comparison between charge and matter distributions. Thus the value of χ^2 for the comparison of theory with the experimental angular distribution has been plotted for each state as a function of the deformation parameter β as shown for example in Fig. 1.

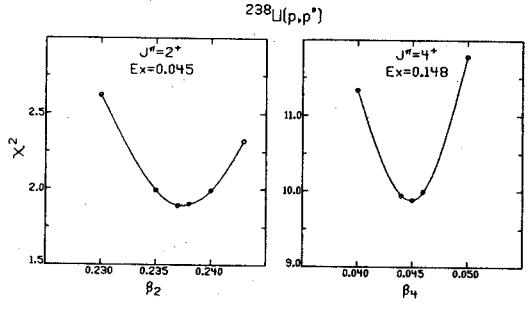

Fig. 1. Sensitivity of the χ^2 fit of inelastic differential cross sections in ^{238}U(p,p') on β_2 and β_4.

In first order, the minimum χ^2 determines the appropriate value of β and the variation of χ^2 with β determines the uncertainty. This method works well for β_2 and β_4 but the χ^2 for the 4+ and 6+ states cannot yet be simultaneously minimized for any value of β_6.

The second direction is the inclusion of spin orbit effects. Recently the code ECIS of J. Raynal which includes spin orbit coupling has been obtained and the coupled channel calculations have been repeated using this code. The results incicate that better fits to all the states including the elastic and 2+ distributions are obtained. (See Fig. 2 for example.) However the values of the β parameters are not changed significantly although the errors are somewhat reduced. Further work on other lanthanide and actinide targets is in progress.

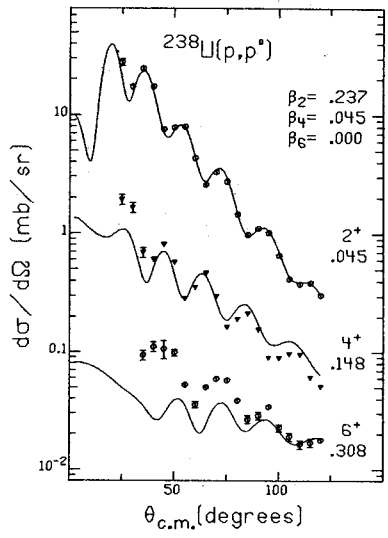

Fig. 2. ^{238}U(p,p') inelastic differential cross sections compared to coupled channel calculations including the spin orbit interaction with "best" fit deformation parameters.

We are also in the process of analyzing the excitation of vibrational states of these same nuclei. The J^π = 2+ and 4+ members of the lowest-lying K=2 band, as well as the lowest-lying members of octupole-vibrational bands, are strongly excited. More weakly excited are members of K=0 bands. Of particular interest will be the quantitative analysis of $J^\pi K = 4^+$ 2 states, which may yield estimates of the contribution of direct E4 transitions to these states. These E4 effects have been long suspected from (d,d')[3] and (α,α')[4] studies. A coupled channels approach will be carried out to provide a consistent analysis of excitations of $I^\pi = 1^-$, 3^-, and 5^- octupole vibrational states. Strengths of E3 transitions are of interest for providing further checks on predictions for both the lanthanide and actinide regions[5].

* Oak Ridge National Laboratory

1. P. Moller, S.G. Nilsson and J.R. Nix, Nucl. Phys. A229 (1974) 292
2. C.H. King, G.M. Crawley, J.A. Nolen, Jr., and J. Finck, J. Phys. Soc. Japan 44 (1978) 564
3. P.O. Tjom and B. Elbek, Nucl. Phys. A107, (1968) 385
4. R.S. Mackintosh, Physics Letters 29B, (1969)629
5. K. Neergard and P. Vogel, Nucl. Phys. A145, (1970) 33 and Nucl. Phys. A149 (1970) 217.

Inelastic Proton Scattering on ^{194,196,198}Pt

P.T. Deason, C.H. King,* T.L. Khoo,** R.M. Ronningen, F.M. Bernthal, and J.A. Nolen, Jr.

Inelastic proton scattering has been performed at this laboratory on several well-deformed nuclides (see G.M. Crawley et al. elsewhere in this report). Because the (p,p') reaction should be especially sensitive to neutron distributions in the nucleus these studies complement and supplement (e,e'), (α,α'), and Coulomb excitation studies. Comparisons between nuclear moments and charge moments are being made as well as an investigation of the effect of the spin-orbit interaction on the deduced moments.

As an outgrowth of our recently completed study of (p,t) reactions in the Pt nuclei, we have been investigating the (p,p') reaction at 35 MeV on ^{194,196,198}Pt. Because these nuclei are in a region where the nuclear shape is slowly changing from prolate to oblate, we hope to exploit the sensitivity of the (p,p') reaction to the nuclear matter deformations to better understand the shapes of the Pt nuclei.

Angular distributions have been measured from 30^{o} to 110^{o} in 5^{o} steps for ≈25 levels in ^{194,196,198}Pt. The protons were detected with nuclear emulsion plates (FWHM ≈5 keV) and with a position sensitive delay-line counter (FWHM ≈20 keV). Angular distributions for the transitions populating the 2_1^+, 2_2^+, 4_1^+, and 4_2^+ levels in ^{196}Pt (p,p') are shown in Fig. 1.

Analyses are being performed using the coupled channels code, ECIS.[1] The proton optical model parameters are those determined by Becchetti and Greenlees,[2] while the initial values for $\beta_2^{N,C}$ and $\beta_4^{N,C}$ are R-scaled values from the work of Baker et al.[3] Fig. 1 shows a preliminary 5-level calculation for ^{196}Pt performed with ECIS. Relative matrix elements were taken from the literature if available, with $P_3<0$, as suggested for ^{194}Pt in Ref. 3 ($P_3=M_{02_1}M_{02_2}M_{2_12_2}$). The unknown matrix elements were taken from the collective model. The calculation reproduces the shapes and strengths of the angular distributions for the 2^+ levels although the calculations for the 2_2^+ level exhibits pronounced minima not seen in the data. Also the calculations for the 4^+ levels predict more structure than seen experimentally and the strength for the 4_2^+ level is underestimated by three orders of magnitude. The strong 4_2^+ transition may in part indicate that a large, direct E4 component is required to explain this strength. Baker et al.[4] suggest this possibility from (α,α') studies of ^{192}Pt. The calculation in Fig. 1 did not include a M_{04_2} matrix element.

The analysis is continuing with the ^{194,198}Pt(p,p') results in addition to investigating the sensitivity of the calculations to the strengths and relative signs of various E2 and E4 components.

---

* Present address: Lawrence Berkeley Laboratory, Berkeley, CA.
** Present address: Argonne National Laboratory Argonne, IL.

1. J. Raynal, unpublished.
2. F.D. Becchetti, Jr., and G.W. Greenlees, Phys. Rev. 182 (1969) 1190.
3. F.T. Baker et al., Nucl. Phys. A266 (1976) 337.
4. F.T. Baker et al., Phys. Rev. C 17 (1978) 1559.

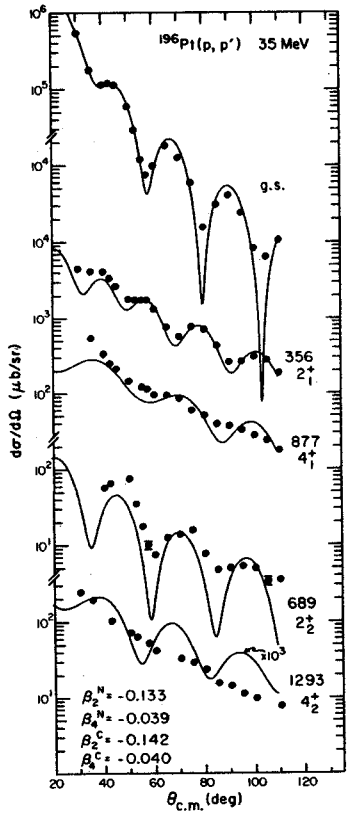

Fig. 1. A 5-level coupled channel calculation performed with ECIS for ^{196}Pt(p,p') with no spin-orbit interaction. Available relative matrix elements were taken from the literature while the remaining values were taken from the collective model. Values for β_2 and β_4 are R-scaled from values in Ref. 3. No direct M_{04_2} matrix element was included.

$^{58}Ni(^{6}Li,^{6}Li')$ at 72 MeV

C. Williamson, A. Galonsky, R. Huffman, and R.G. Markham

The $^{58}Ni(^{6}Li,^{6}Li')$ reaction at a bombarding energy of 72 MeV is being used to resolve or reduce optical model ambiguities from the elastic scattering experiment done by Huffman, et al. (see elsewhere in this annual report).

A delay-line, position-sensitive proportional counter, backed by a scintillator, placed in the focal plane of the Enge split-pole spectrograph was used to gather the spectra. The low intensity of 10-20 nA (on target) of the ^{6}Li beam restricted the range over which it was possible to gather data to angles less than approximately 45^{o}. It was possible to resolve six inelastic states (see Fig.1) through the entire angular range for which data were obtained. With this set-up, we were able to obtain ∿90 keV FWHM resolution.

After trying a second set of optical model parameters in the code DWUCK 72, we were able to produce the preliminary fits to data shown in Fig. 2. However we have not yet completed searches for optical model parameters which fit the elastic data. It is possible that these future searches may provide a more acceptable fit to the inelastic data.

One motivation for performing this experiment was to compare values of deformation lengths βR determined by $(^{6}Li,^{6}Li')$ with (p,p'), (α,α') etc. Various methods for explaning the difference between βR values obtained by nuclear excitation and Coulomb excitation have been put forth in the past[3,4] and use of these methods was expected to be necessary. In their studies of $^{6}Li + ^{90}Zr$, Pardo et al.[1] obtained a value for β^2 which was only 0.36 of the accepted values. It was felt that similar discrepancies might be observed for the ^{58}Ni nucleus. The results of the work on ^{58}Ni, along with the accepted values, are shown in Table 1. The accepted values are taken from A.M. Bernstein[2]. No difference between these values has been found to date.

Finally, use of a double folding model code developed by F. Petrovich and D. Stanley[5] will be used for analysis of this reaction. It is thought that the double folding model will fit the inelastic data in the small angle region better than the optical model.

Table 1. Values of βR obtained in this work and corresponding accepted values[2]. $R=r_{o}A^{1/3}$ where the radius of the real well (r_{o}=1.40 fm) of the optical model was used.

J^{π}	2^{+}	3^{-}	4^{+}
Energy	1.454	4.475	4.754
βR(fm) this work	1.15	0.77	0.30
βR(fm) accepted	1.03±.05	0.82±.06	

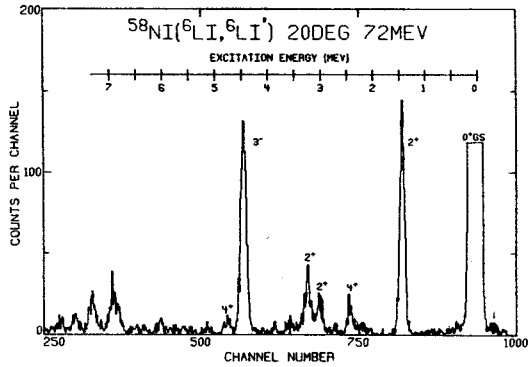

Fig. 1. Typical spectrum showing inelastic states which may be resolved through the entire range for which data was taken.

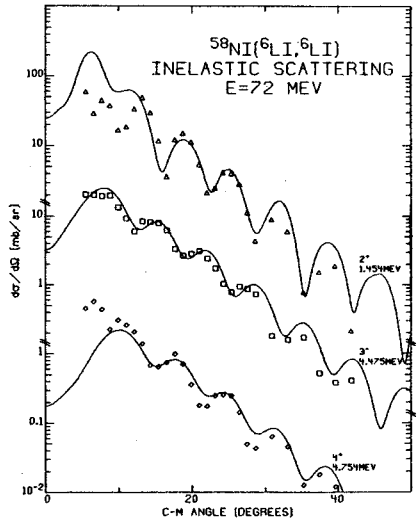

Fig. 2. Angular distributions obtained in this experiment. The smooth curves are DWBA fits to the data.

1. R. Pardo, R.G. Markham, W. Benenson, A.I. Galonsky, E. Kashy, Physics Letters 71B (1977) 301.
2. A.M. Bernstein, Advances in Nuclear Physics Baranger and Vogt, Plenum Press, NY, 1962, p. 427.
3. D.L. Hendrie, Phys. Rev. Letters 31 (1973) 478.
4. W.J. Thompson, J.S. Eck, Phys. Letters 67B (1977) 151.
5. F. Petrovich, D. Stanley, Nucl. Phys. A275 (1977) 487.

The Nuclear "Coupling Constant" for Analogs of Gamow-Teller Transitions in Charge Exchange Reactions--A Measurement at 25, 35, and 45 MeV Using the $^{7}Li(p,n)^{7}Be$ Reaction

L.E. Young, S.M. Austin, R.R. Doering, R. DeVito, R.K. Bhowmik, and S.D. Schery

Several studies[1] have taken advantage of the strong resemblance between the charge exchange operator $V_{\sigma\tau}(\vec{\sigma}_i \cdot \vec{\sigma}_p)(\vec{\tau}_i \cdot \vec{\tau}_p)$ and the Gamow-Teller (GT) or M1 operators to search for Gamow-Teller strength or analogs of M1 strength using (p,n) reactions. To make these studies quantitative it is necessary to know the relevant nuclear "coupling constant" $V_{\sigma\tau}$ and the strength of the tensor force $V_{T\tau}$ which also flips spin and isospin. Unfortunately nearly all empirical information about these quantities is obtained from studies of very light nuclei[2] and is subject to large optical model and reaction mechanism uncertainties.

We describe here measurements at bombarding energies of 25, 35, and 45 MeV, of cross sections for the $^{7}Li(p,n)^{7}Be$ reaction leading to the ground ($3/2^-$) and first excited (429 keV, $1/2^-$) states of ^{7}Be. Since $V_{\sigma\tau}$ dominates the reaction to the 429 keV state while both $V_{\sigma\tau}$ and the operator $V_\tau(r)\vec{\tau}_i \cdot \vec{\tau}_p$ are important for the ground state, an analysis of the ratio of cross sections to these states yields the ratio $V_{\sigma\tau}/V_\tau$ with much of the model dependence hopefully vanishing in the ratio. V_τ is relatively well known in this energy range,[3] allowing one to calculate $V_{\sigma\tau}$.

Measurements were carried out with the MSU beam swinger time-of-flight facility. Flight paths up to 30 meters and an overall time resolution between 0.55 and 0.8 nsec permitted clean separation of the ground and first excited states at all energies. The ratios of the cross sections at 35 MeV are shown in Fig. 1.

Initial analysis has been in terms of the model of Anderson et al.[4] assuming that only central forces (no tensor) contribute to the reaction and that only L=0 transfer is important. In this limit the necessary nuclear structure information can be obtained from β-decay ft values and one obtains

$$\frac{\sigma_1}{\sigma_0} = \frac{1.14\ V_{\sigma\tau}^2}{V_\tau^2 + 1.34\ V_{\sigma\tau}^2} = \frac{1.14}{(V_\tau/V_{\sigma\tau})^2 + 1.34} \qquad (1)$$

The results of this analysis are shown in Table I and are in good agreement with previous results.

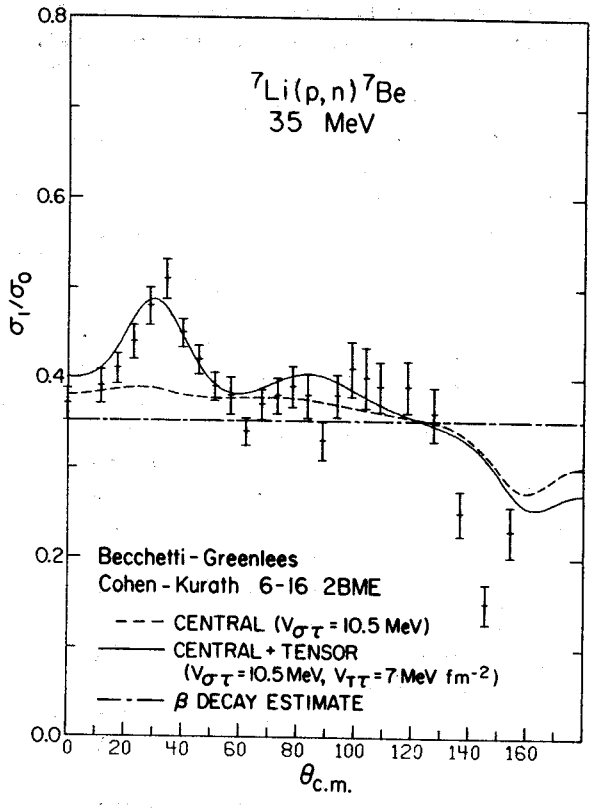

Fig. 1. Ratio of cross sections σ_1/σ_0 at E_p=35 MeV. The DWBA calculations shown were performed using Becchetti and Greenlees "best fit" optical model potentials, the wavefunctions of Cohen and Kurath (6-16 2BME matrix elements) and forces noted. For more details, see text.

The data at 35 MeV have also been analyzed in the distorted wave approximation. Several sets of wave functions, optical model potentials, and effective interactions, the latter including G-matrix[5] and empirical[2] interactions, were tried. While the individual cross sections varied as much as a factor of two for these different choices, the cross section ratio was much less affected. The dashed curve shown in Fig. 1 is the result of a particular calculation for an empirical central force (V_o=-27 MeV, V_σ=+9 MeV, V_τ=15.5 MeV, $V_{\sigma\tau}$=10.5 MeV). It is typical of all such calculations in that the ratio is nearly independent of angle and does not reproduce the peak in the cross section near 40°. The solid curve in Fig. 1 was obtained by adding a tensor force of an r^2x (Yukawa) radial form:

$$V_{T\tau}(r) = V_{T\tau} r^2 \frac{e^{-r/\mu}}{r/\mu} S_{12} \vec{\tau}_i \cdot \vec{\tau}_p$$

where μ=0.816 fm [2] and S_{12} is the usual tensor operator. No other way was found to reproduce the peak and this ratio measurement appears therefore to be the best present evidence for a tensor force in this energy range. Shown as a dotted line is the ratio predicted by eq. 1 for the β decay ft values implicit in the Cohen Kurath wavefunctions.

The values $V_{\sigma\tau}$=10.5 MeV, $V_{T\tau}$=7 MeV fm^{-2} obtained here agree reasonably well with those obtained in recent G-matrix fits[5] to the two nucleon data, and are perhaps the most reliable estimates of $V_{\sigma\tau}$ and $V_{T\tau}$ available.

Finally, it is perhaps worth pointing out that the value of $V_{\sigma\tau}$ appears to increase somewhat over the 25-45 MeV range. This trend is consistent with the theoretical expectations[6] and with the dominance of transitions mediated by $V_{\sigma\tau}$ over those mediated by V_τ noted in measurements near 140 MeV.[7]

1. R.R. Doering et al., Phys. Rev. Lett. 35 (1975) 691; U.E.P. Berg et al., B.A.P.S. 23 (1978) 520.
2. S.M. Austin in The Two-Body Force in Nuclei, Plenum Press, 1972, p. 285.
3. R.R. Doering, D.M. Patterson, and A. Galonsky, Phys. Rev. C 12 (1975) 378.
4. J.D. Anderson, C. Wong, and V.A. Madsen, Phys. Rev. Lett. 24 (1970) 1074.
5. G. Bertsch et al., Nucl. Phys. A284 (1977) 399.
6. G. Love, private communication.
7. C.D. Goodman et al., B.A.P.S. 23 (1978) 526.

Table I. Values of $V_{\sigma\tau}$ for a 1 fm range Yukawa Interaction.

E_p	σ_o/σ_1	$V_\tau/V_{\sigma\tau}$	V_τ	$V_{\sigma\tau}$
24.8[1]	2.83	1.46	17.0	12.4
35[1]	2.45	1.28	15.3	12.7
45[1]	2.17	1.13	14.6	13.7
35[2]				10.5

1. From analysis using eq. 1.
2. From DWBA analysis with $V_{T\tau}$ = 7 MeV fm^{-2}.

Comparative Studies of the (p,n) Reaction on $^{24,25,26}Mg$

U.E.P. Berg, S.M. Austin, A.I. Galonsky, R. DeVito, Y. Iwasaki, and L.E. Young

Introduction

The (p,n) reaction on light nuclei can provide a variety of information concerning the charge exchange reacion mechanism and the relationship between Fermi and Gamow-Teller strength and charge exchange cross sections. Values for the isospin flip and isospin-spin flip two body interactions V_τ and $V_{\sigma\tau}$ and perhaps the tensor interaction can be obtained from an analysis of angular distributions in terms of a distorted wave approximation. We have studied the (p,n) reaction on $^{24,25,26}Mg$ to investigate the influence of valence neutrons on these transitions. Further points of interest were to determine experimentally the relative excitation of different multipolarities in (p,n) reactions and to test the applicability of an energy-dependent Lane-model nucleon-nucleus optical potential[1] for transitions to isobaric analog states (IAS) in ^{25}Mg and ^{26}Mg.

Experiment

The experiments were performed at the neutron time of flight setup using a 35 MeV proton beam incident on 5 mg/cm^2 isotopically enriched (99%) $^{24,25,26}Mg$ targets. Angular distributions from 7° to 120° were taken at a 22.48 m flight path for all three targets. The maximum available flight path was chosen for a measurement at 30° with better energy resolution. The energy resolution was 180 keV for 30 MeV neutrons (from IAS in $^{25,26}Mg$) and 90 keV for 20 MeV neutrons (from the ground state in ^{24}Al, Q=−14.665 MeV). The proton beam was swept at a rate allowing one of five (one of three for 22.48 m) beam bursts to reach the target. This allowed the observation of neutrons in a dynamic range from 14 to 30 MeV.

Fig. 1 shows a comparison of the measured neutron time of flight spectra. The energy threshold was 5.95 MeV (electron energy corresponds to 10 MeV neutron energy), and the spectra were gated by the neutron peak from a γ-ray-neutron pulse shape discrimination spectrum. Prominent structure is observed even for highly-excited states in the continuum of these nuclei. This condition allows an analysis of the angular distribution for individual states. The $^{24}Mg(p,n)^{24}Al$ spectrum is shifted to lower energy by the high negative Q-value for this reaction. This permits one to use neutrons from well-known states in ^{24}Al to determine excitation energies of the highly excited states in ^{25}Al and ^{26}Al within ±30 keV. The $^{25,26}Mg(p,n)$ spectra at forward angles are dominated by the transition to the iosbaric analog state. The strengths to these IAS amount to 31% and 21% of the total ^{25}Mg and $^{26}Mg(p,n)$ strengths observed at 30°. The presence of one or two valence neutrons outside the ^{24}Mg "core" causes a rise of the (p,n) cross section. The cross section ratios at 30° (for states up to 15 MeV excitation energy) in $^{24,25,26}Al$ are 1:1.6:2.8, respectively.

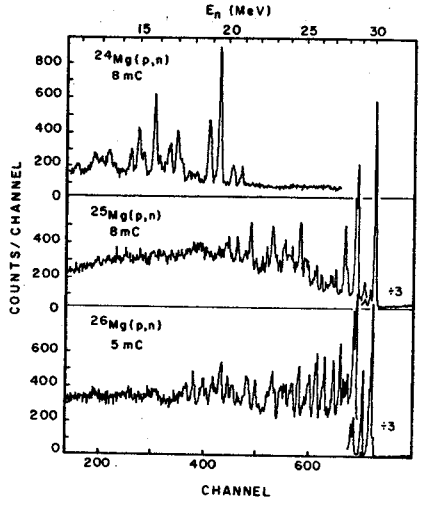

Fig. 1. Neutron time-of-flight spectra from the (p,n) reaction on $^{24,25,26}Mg$. The flight path was 32 m, proton energy 35 MeV, and scattering angle 30°. These spectra were gated by a light threshold of 2.5 times ^{228}Th Compton edge (5.95 MeV electron energy) and by the neutron peak of the pulse shape discrimination spectrum.

Optical-Model Analysis of the Quasielastic Scattering

Patterson et al.[1] obtained a Lane-model optical potential from a fit to (p,n) isobaric analog state (IAS) data using an imaginary surface energy-dependent isovector strength added to the Becchetti-Greenlees Coulomb-corrected proton parameter set.[2] We have tested the applicability of these optical-potential parameters by comparing our measured angular distributions for the $^{25,26}Mg(p,n)$ IAS transitions with DWBA calculations using these Lane-model optical potential parameters.

The $^{25,26}Mg(p,n)^{25,26}Al$ spectra are dominated by the iosbaric analog state transition at forward angles, but at backward angles for ^{26}Mg the (p,n) transition to the IAS at E_x=228 keV in ^{26}Al has a smaller cross section than the transitions to the ground (4^+) and 417 keV (3^+) state. Since these three peaks overlap it was necessary to extract the individual cross sections by peak-fitting the spectra. A peak-fitting routine was written which calculates the supposed peak positions and peak form from an isolated reference peak by using a previously determined time calibration and determining the neutron energies from the proton beam energy and reaction kinematics.

Fig. 2 shows the measured angular distributions for the $^{25,26}Mg(p,n)$ IAS transitions, together with calculated angular distributions using

the computer code DWUCK. The optical-model parameters, obtained from Ref. 1, set B, are given in Table I.

Table I. Lane-model optical potential parameters from Ref. 1 used for DWBA calculations in Fig. 2. The quantities used in this table are explained in Ref. 1. r_R=1.17 fm, a_R=0.75 fm, r_I=1.32 fm, $V_{s.o.}$=6.2 MeV, $r_{s.o.}$=1.01 fm, and $a_{s.o.}$=0.75 fm.

	V(MeV)	4xWS(MeV)	W(MeV)	a_I(fm)
^{25}Mg(p,n)				
Interaction	1.4	2.6	---	.54
Proton	46.4	12.0	5.5	.54
Neutron	46.9	13.5	5.2	.48
^{26}Mg(p,n)				
Interaction	1.9	3.9	---	.56
Proton	47.1	13.1	5.5	.56
Neutron	46.1	11.8	5.2	.51

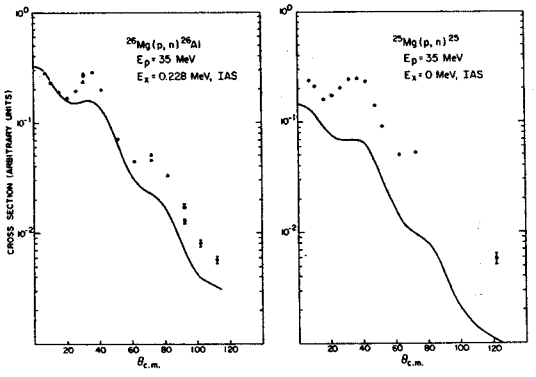

Fig. 2. Angular distributions for the quasi-elastic (p,n) reaction on ^{25}Mg and ^{26}Mg. The DWBA calculations and measured data have been normalized at the (relative) ^{26}Mg(p,n) cross section at forward angles (θ_{cm}=7.3° and 10.4°).

The calculations are in fair agreement with the measurements. Maxima and minima of the angular distributions are predicted correctly, but the calculations yield a steeper negative slope with increasing angle. The IAS angular distributions for both nuclei are essentially the same (perhaps a little more structured for ^{26}Mg). The measured quasielastic cross section for ^{25}Mg is within 10% of the corresponding ^{26}Mg(p,n) cross section, while the calculation gives a decrease by a factor of 2.2 for the ^{25}Mg cross section.

Giant Gamow-Teller Transitions

The pure isospin part of the nucleon-nucleon interaction V_τ is responsible for the large (p,n) cross section to isobaric analog states (IAS). In IAS transitions (Fermi-like transitions) a valence neutron is simply replaced by a proton. No IAS of the ^{24}Mg ground state can be excited because of its isospin T=0; a simple replacement of a neutron by a proton is forbidden by the Pauli principle. Although a (p,n) reaction on ^{24}Mg is a direct reaction, it causes a more complicated rearrangement of nucleons to form a T=1 nucleus. One possible rearrangement is a spin flip transition from the $d_{5/2}$ into the $d_{3/2}$ shell forming a 1^+ state. Strong M1 transitions in ^{24}Mg are well known from inelastic electron[3] and photon scattering,[4] and one would expect to excite the analog states of the giant magnetic dipole resonance in ^{24}Mg through the isospin-spin-flip part of the nucleon-nucleon interaction $V_{\sigma\tau}$. These Gamow-Teller excitations of the ^{24}Mg core must also be possible for ^{25}Mg and ^{26}Mg; but here the valence neutrons can couple to the 1^+ core configuration leading to 3/2, 5/2, and 7/2 states in ^{25}Al or to 1^+ states in ^{26}Al.

We looked for Gamow-Teller strength observed in the ^{24,25,26}Mg(p,n) reaction by comparing our data with results from (e,e')[3] and (γ,γ)[4] measurements. Two strong M1 transitions are known in ^{24}Mg. The strongest (p,n) transition occurs to a state at 1.12 MeV in ^{24}Al, which is presumed to be the analog of the 1^+ state in ^{24}Mg having the largest M1 ground state decay strength. Unfortunately, the 1.12-MeV peak is a doublet (1^+,2^+) of 20-keV spacing which is not resolved in our experiment, but an analysis of the angular distribution indicates that the strength is dominated by a transition to a 1^+ state. The transition to the second strongest 1^+ state was also observed. There are indications from earlier electron scattering work done at Darmstadt[5] and from shell model calculations performed at MSU[6] that further M1 strength will be found in states between 12 and 15 MeV in ^{24}Mg. The angular distributions of the strong transitions in the analogous excitation region from 3 to 6 MeV in ^{24}Al are being analyzed to test this point.

The situation for ^{25}Mg(p,n)^{25}Al is more complicated because Gamow-Teller-like transitions can lead to 7/2, 5/2, and 3/2 states. The measured spectra show that strong transitions are visible in regions where considerable M1 strength in ^{25}Mg(e,e') was found. One of the strongest transitions leads to the first T=3/2 states in ^{25}Al.

We examine the case of ^{26}Mg(p,n) in more detail. Fig. 3 shows that part of the ^{26}Mg(p,n) spectrum, where one expects to find analog states of the giant M1 resonance in ^{26}Mg. The spectrum has been recorded at 30° and a flight path of 22.48 m. The background has been subtracted. Each labeled state has the angular distribution of a 1^+ state (see Fig. 4) and an excitation energy close to 1^+ states observed in ^{26}Mg. B(M1) values obtained from (e,e') at 180° are shown in Fig. 3 for comparison with the (p,n) spectrum. The ratios of the peak areas approximate closely

the ratios of the B(M1) values. On the other hand, a discrepancy at 13.3 MeV, where we observe no (p,n) strength, is obvious.

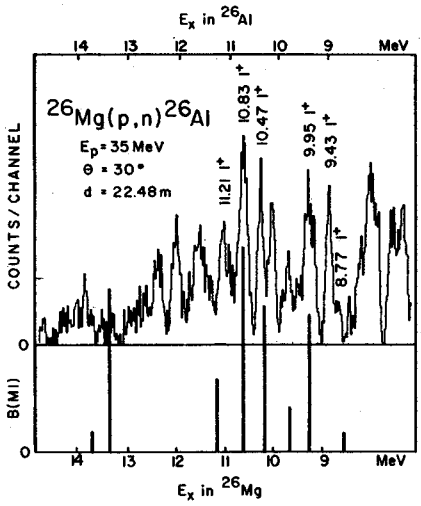

Fig. 3. Comparison between Gamow-Teller transitions observed in ^{26}Mg(p,n)^{26}Al and B(M1) values from (e,e').[3] The energy scales have been aligned at the isobaric analog of the ground state at 228 keV in ^{26}Al.

Fig. 4 shows a comparison of the measured angular distributions of the two strongest transitions (10.83 and 10.47 MeV) together with an angular distribution to a strong and isolated 1^+ state at 1.058 MeV excitation energy. It seems reasonable to conclude from this comparison that the states involved have spin and parity 1^+. The measured angular distribution for the 0^+ IAS, which is also reached by ℓ=0 transfer, is obviously different (see Fig. 2) from the 1^+ states angular distribution and, furthermore, the transitions with ℓ=2 transfer show a different slope.

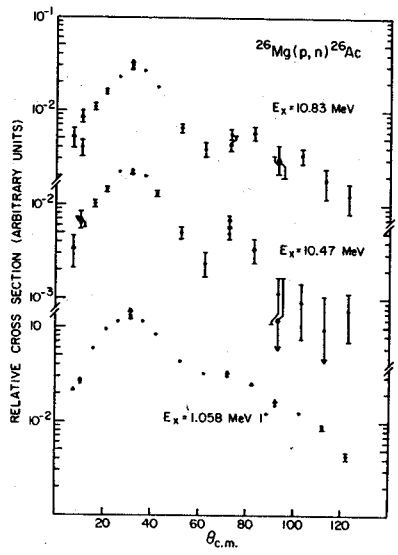

Fig. 4. Comparison of angular distributions to 1^+ states (see text).

Further analysis of the data will include microscopic DWBA calculations using the full-sd-shell model transitions densities of Chung and Wildenthal[6] and a determination of spins of the high-energy states observed which so far are unknown.

---

1. D.M. Patterson, R.R. Doering, and Aaron Galonsky, Nucl. Phys. A263 (1976) 261.
2. F.D. Becchetti, Jr. and G.W. Greenlees, Phys. Rev. 182 (1969) 1190.
3. L.W. Fagg, Rev. Mod. Phys. 47 (1975) 683.
4. U.E.P. Berg, K. Wienhard, and H. Wolf, Phys. Rev. C 11 (1975) 1851.
5. O. Titze and E. Spamer, Z. Naturforschung 21a (1966) 1504.
6. W. Chung and B.H. Wildenthal, private communication.

(^{3}He,t) Charge-Exchange Scattering at 130 MeV

A. Galonsky, H. Sarafian, J.-P. Didelez,* A. Djaloeis,* and W. Oelert*

Charge-exchange scattering, that is, scattering to the iosbaric analogue state of the target, has been performed at Jülich with 130-MeV helions on targets of ^{90}Zr, ^{120}Sn, and ^{208}Pb. The angular distributions have been analyzed with the aid of the direct-reaction code DWUCK in an attempt to find systematics in the mass 3-nucleus isovector potential.

The number of free parameters was intentionally limited by imposing upon the isovector potential the same geometry as determined in analyses of ^{3}He elastic scattering utilizing Woods-Saxon potential shapes. This restriction left only the strengths of the real and imaginary parts to be determined. Once the optical potential was chosen, the shape of the (^{3}He,t) angular distribution was determined only by the ratio of these strengths, say V_1/W_1. The absolute value of the angular distribution then scaled as the square of one strength, say W_1^2. By trial-and-error eyeball fitting to the data the two strengths were determined.

The data and some of the better fits are shown in the three figures. In each figure, the dashed curve was obtained with the optical-model parameters of Fulmer et al.[1] These parameters are based upon 70-MeV data; the imaginary potential is surface-peaked. The solid curves are better fits to the data. They employed an optical potential[2] based upon 130-MeV data taken simultaneously with the (^{3}He,t) data; the imaginary part is of the volume form.

The values of V_1 and W_1, the real and imaginary isovector strengths, are given below.

Table I.

	Fulmer OM-Dashed Curves		Djaloeis OM-Solid Curves	
	W_1(MeV)	V_1/W_1	W_1(MeV)	V_1/W_1
^{90}Zr	8	0	12	1.4
^{120}Sn	10	.4	9	.01
^{208}Pb	6	0	7	.14

Undoubtedly because of its larger radius, the imaginary part of the isovector potential is mainly responsible for the charge-exchange cross section. This was true even for the ^{90}Zr solid curve, where V_1/W_1=1.4. Inclusion of the V_1 part improves the quality of the relative fit but makes little difference in fixing the absolute value. Hence, with the geometries used here, the value of W_1 may be taken as the strength of the interaction. That strength appears to be somewhat independent of optical-model potential and of target nucleus, and to have the value $W_1 \simeq 8$ MeV.

One of our targets, ^{90}Zr, has been studied at lower bombarding energies. Using a modified Fulmer geometry in the isovector potential, Hinrichs and Show[3] fitted data at 37.5 MeV and at 70 MeV and found $W_1 \simeq 14$ MeV and 4 MeV, respectively. With the same modification we find $W_1 \simeq 4$ MeV at 130 MeV, implying a more constant isovector potential at the higher projectile energies.

* Institut für Kernphysik, KFA-Jülich.

1. C.B. Fulmer, J.C. Hafele, and C.C. Foster, Phys. Rev. C 8 (1973) 200.
2. A. Djaloeis, J.-P. Didelez, A. Galonsky, and W. Oelert, submitted to Nuclear Physics.
3. R.L. Hinrichs and D.L. Show, Phys. Rev. C 6 (1972) 1257.